JACS
JOURNAL OF THE AMERICAN CHEMICAL SOCIETY
Article
pubs.acs.org/JACS

Partially Hydrated Electrons at the Air/Water Interface Observed by UV-Excited Time-Resolved Heterodyne-Detected Vibrational Sum Frequency Generation Spectroscopy

Korenobu Matsuzaki,[†,‡,⊥] Ryoji Kusaka,[†,∥] Satoshi Nihonyanagi,[†,§] Shoichi Yamaguchi,[†,§,#] Takashi Nagata,[‡] and Tahei Tahara*[,†,§]

[†]Molecular Spectroscopy Laboratory, RIKEN, 2-1 Hirosawa, Wako, Saitama 351-0198, Japan
[‡]Department of Chemistry, School of Science, The University of Tokyo, 3-8-1 Komaba, Meguro-ku, Tokyo 153-8902, Japan
[§]Ultrafast Spectroscopy Research Team, RIKEN Center for Advanced Photonics (RAP), RIKEN, 2-1 Hirosawa, Wako, Saitama 351-0198, Japan

Supporting Information

ABSTRACT: Hydrated electrons are the most fundamental anion species, consisting only of electrons and surrounding water molecules. Although hydrated electrons have been extensively studied in the bulk aqueous solutions, even their existence is still controversial at the water surface. Here, we report the observation and characterization of hydrated electrons at the air/water interface using new time-resolved interface-selective nonlinear vibrational spectroscopy. With the generation of electrons at the air/water interface by ultraviolet photoirradiation, we observed the appearance of a strong transient band in the OH stretch region by heterodyne-detected vibrational sum-frequency generation. Through the comparison with the time-resolved spectra at the air/indole solution interface, the transient band was assigned to the vibration of water molecules that solvate electrons at the interface. The analysis of the frequency and decay of the observed transient band indicated that the electrons are only partially hydrated at the water surface, and that they escape into the bulk within 100 ps.

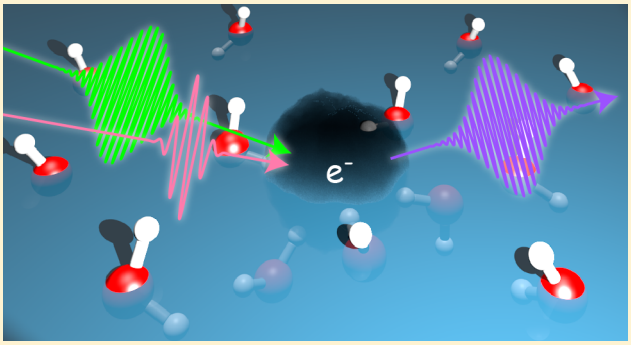

INTRODUCTION

When an electron is released into water, the hydrated electron is formed. This simplest anionic species consists of only one electron and several solvating water molecules, and has been intensively studied[1−9] because of its crucial role in a variety of chemical/physical/biological processes.[10] Although the reactions of hydrated electrons are particularly important at interfaces where hydrated electrons encounter chemical species in the other phase, the properties of hydrated electrons at interfaces are still poorly understood. So far, two studies claim to have observed hydrated electrons at the air/water interface: A photoelectron study using a liquid water jet claim that the electrons are half hydrated at the interface,[11] whereas a second harmonic generation (SHG) study at the air/water interface conclude that the electrons are fully hydrated.[12] Their conclusions differ from each other, and in fact, even the existence of electrons at the water surface has not been established yet.[13]

Heterodyne-detected vibrational sum frequency generation (HD-VSFG) spectroscopy has recently emerged as a powerful technique for the steady-state characterization of interfaces.[14,15] VSFG is a second-order nonlinear optical process that allows us to selectively obtain the vibrational spectra of an interfacial layer as thin as 1 nm. With the heterodyne detection, HD-VSFG enables the direct determination of the phase and amplitude of the second-order nonlinear susceptibility ($\chi^{(2)}$), which provides vibrational spectra at aqueous interfaces for direct comparison with vibrational spectra in the bulk.[16−19] The combination of HD-VSFG spectroscopy and the pump−probe method[20−27] is ideal for characterizing hydrated electrons transiently generated at the air/water interface. Here we report the observation and characterization of hydrated electrons at the air/water interface by UV-excited time-resolved HD-VSFG spectroscopy which was developed for this study.

EXPERIMENTAL SECTION

Materials. Air/water and air/indole solution interfaces were used as the sample. For the air/water interface, high purity water (18.2 MΩ·cm resistivity) obtained from a commercial water purification system (Millipore, Milli-Q Advantage A10) was used as it is. For the air/indole solution interface, 17 mM indole aqueous solution was prepared by dissolving indole (purity >99.0%, Tokyo Chemical

Received: November 18, 2015
Revised: February 27, 2016
Published: June 9, 2016

DOI: 10.1021/jacs.6b02171
J. Am. Chem. Soc. 2016, 138, 7551−7557

Industry) in the high-purity water with approximately 5 h of sonication. The temperature of both of the liquid samples during the measurements was kept at the room temperature (24−25 °C).

UV-Excited Time-Resolved HD-VSFG Spectroscopy. A new setup was developed to perform UV-excited time-resolved heterodyne-detected vibrational sum frequency generation (HD-VSFG[16]) experiments in this study (Figure 1). In this setup, a commercial Ti:sapphire

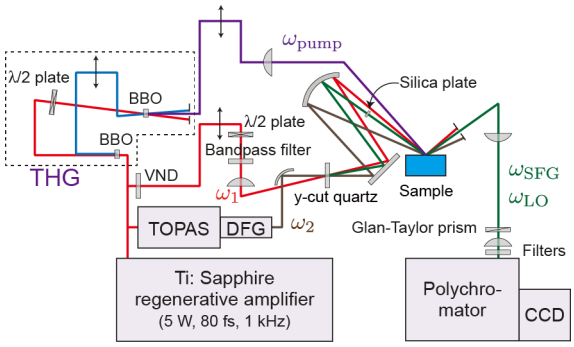

Figure 1. Schematic of the UV-excited time-resolved HD-VSFG spectrometer developed in the present study to perform the detection and characterization of short-lived transient species at air/liquid interfaces.

regenerative amplifier (Spectra Physics, Spitfire Ace) was used as the light source which generates 800 nm pulses (5 mJ, 80 fs) at the repetition rate of 1 kHz. Of the output, 1 mJ was attenuated by a variable neutral density (VND) filter and spectrally narrowed by a bandpass filter (center wavelength, 795 nm; bandwidth, 20 cm^{-1}) to be used as the narrow band visible light, ω_1. Another 2 mJ was converted to a tunable and broadband infrared beam (ω_2) using a commercial optical parametric amplifier with a difference frequency generation unit (Spectra Physics, TOPAS-C). Using these ω_1 and ω_2 beams, the HD-VSFG measurement was carried out in the following way. First, ω_1 and ω_2 beams were focused into a thin crystal of y-cut quartz (thickness, 10 μm), where the local oscillator (ω_{LO}) was generated by the sum frequency mixing of ω_1 and ω_2. A plano-convex lens (f = 500 mm) and an off-axis parabolic mirror (f = 100 mm) were used for focusing ω_1 and ω_2, respectively. The generated local oscillator and the transmitted ω_1 and ω_2 beams were then refocused by a spherical concave mirror onto the sample surface. The incident angle and the polarization direction were ∼40° and S for ω_1, and ∼50° and P for ω_2. In this process, ω_{LO} was transmitted through a silica plate of 3 mm thickness, causing it to be delayed by about 5 ps with respect to ω_1 and ω_2 beams. At the sample surface, VSFG took place and generated the sum frequency light (ω_3). The S-polarized component of ω_3 and ω_{LO} was isolated by a Glan-Taylor prism, and the two beams were collinearly introduced into a polychromator. Inside the polychromator, ω_3 and ω_{LO} were frequency dispersed and detected by a liquid nitrogen cooled charge coupled device (CCD; Princeton Instruments, Spec-10). The interference pattern recorded on the CCD was analyzed in a similar manner to that we previously reported to obtain the complex second-order nonlinear susceptibility, $\chi^{(2)}$.[16,28] The phase and amplitude calibration was done using quartz as the reference.

In the time-resolved measurements, the remaining 2 mJ of the regenerative amplifier output was converted to the UV pump light (ω_{pump}) at 267 nm. In this process, the fundamental light at 800 nm was first converted to the second harmonic light at 400 nm in a β-barium borate (BBO) crystal (CASTECH, Type I, thickness: 1 mm). The third harmonic light at 267 nm was then generated by sum frequency mixing of the fundamental and the second harmonic beams in another BBO crystal (CASTECH, Type I, thickness: 1 mm) after optimizing the temporal overlap between the two beams. The UV pump light generated in this manner was focused onto the sample surface using a plano-convex lens (f = 350 mm) with the incident angle of 25° and with the P-polarization, and the change of $\chi^{(2)}$ ($\Delta\chi^{(2)}$) caused by the pump light was evaluated as the transient spectrum. The pump−probe delay of the transient spectrum is determined by the temporal separation between ω_2 and ω_{pump} pulses, because the pulse duration of ω_2 (∼100 fs) is much shorter than that of ω_1 (∼1 ps). This temporal separation was adjusted by a computer-controlled delay stage. The instrumental response was determined from the rising time of $\Delta\chi^{(2)}$ of a ZnO crystal, and the fwhm of the fitted Gaussian function was 130 fs. Pump light intensity was adjusted to be 25 mW for the air/water interface, and 5 mW for the air/indole solution interface. At the air/water interface, the pump light was focused more tightly than at the air/indole solution interface to make the two-photon absorption more efficient. When the UV-pump light is used, the accumulation of the photodegraded sample at the sample surface becomes problematic. This was avoided by continuously flowing the sample solution during the measurements while the sample surface was kept at the same height throughout the measurement with the accuracy of about 1 μm, which is the requirement for a successful HD-VSFG measurement.[16,28] The typical acquisition time of transient spectra at each delay was ∼10 min.

RESULTS AND DISCUSSION

Air/Water Interface. The steady-state interface-selective spectrum (where Im $\chi^{(2)}$ is the imaginary part of the second-order nonlinear susceptibility) of the air/water interface is shown in Figure 2a. A positive band at ∼3700 cm^{-1} and a

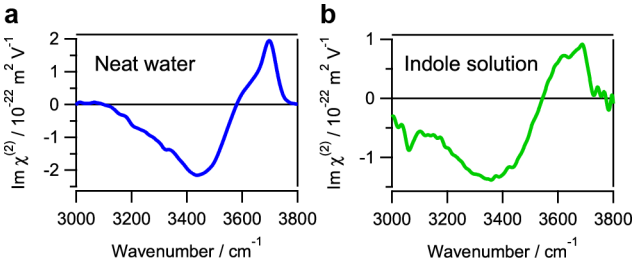

Figure 2. Steady-state Im $\chi^{(2)}$ spectrum (a) at the air/water interface and (b) at the air/indole solution interface.

negative band at ∼3450 cm^{-1} are clearly observed, which are assignable to the OH stretch vibrations of the free OH group and the hydrogen-bonded OH group, respectively.[29−31] We note that the positive band below 3200 cm^{-1}, which was reported in previous HD-VSFG studies,[16,31] does not appear in this spectrum. In fact, our recent studies have shown that no noticeable positive vibrational resonance exists in this region within the S/N, and the previously reported band is likely an artifact due to inaccurate phase calibration.[30,32]

When the sample surface is irradiated with 267 nm pump light, electrons are generated through the two-photon ionization of water,[5]

$$H_2O \xrightarrow{2h\nu,\ H_2O} OH^{\bullet} + H_3O^{+} + e^{-} \quad (1)$$

Figure 3 shows the UV-pumped time-resolved interface-selective spectra, Im $\Delta\chi^{(2)}$ = Im[$\chi^{(2)}(t) - \chi^{(2)}{}_0$], in the OH stretch region at the air/water interface. ($\chi^{(2)}(t)$ and $\chi^{(2)}{}_0$ are the second-order nonlinear susceptibilities in the presence of UV light at delay t and in the absence of UV light, respectively.) In these transient spectra, the 3050−3400 and 3400−3800 cm^{-1} ranges were measured separately, and they are connected using the same scaling factor for all the delays. As readily seen in this figure, a very strong positive transient band at around 3260 cm^{-1} and a broad positive offset appear with UV irradiation, and they decay almost completely within 100 ps. The decay is monotonic, and no appreciable change in the

DOI: 10.1021/jacs.6b02171
J. Am. Chem. Soc. 2016, 138, 7551−7557

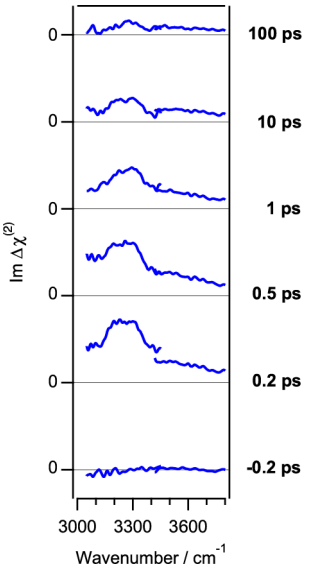

Figure 3. Time-resolved Im $\chi^{(2)}$ spectra (Im $\Delta\chi^{(2)}$) of the air/water interface. The spectrum at −0.2 ps provides an estimate of the noise in our spectra. The spectra in the low and high wavenumber ranges were measured separately, and they are connected using the same scaling factor for all the delays.

spectral shape is observed, indicating that the time-resolved spectra are represented by only one component (Figure 4a). The temporal change of this transient is obtained by plotting the integrated intensity of the spectra at each delay, and it is depicted in Figure 4b. The transient component rises almost instantaneously and then shows a nonexponential decay on a 10 ps time scale. The intensity of the transient band is very high, and is comparable to the OH stretch band intensity in the steady-state spectrum. Actually, the transient signal appears without any noticeable bleach of the steady-state signal, which should give a positive broad bleach that is peaked around 3450 cm^{-1} and disappears below 3100 cm^{-1} as expected from the steady-state spectrum shown in Figure 2a. Furthermore, we did not observe any bleach signal due to the free OH band at 3700 cm^{-1} either, which should appear as a sharp negative band. The absence of the bleach signal implies that the observed transient signal originates from a very small number of water molecules. Thus, the time-resolved spectra clearly show that the UV pump light generates a transient species exhibiting a very large VSFG signal in the OH stretch region at the water surface.

In order to confirm that the transient species is generated by eq 1, we evaluated the pump power dependence of the transient signal intensity. Since eq 1 involves two-photon excitation, we expect a quadratic power dependence. The filled circles in Figure 5a show the experimentally determined

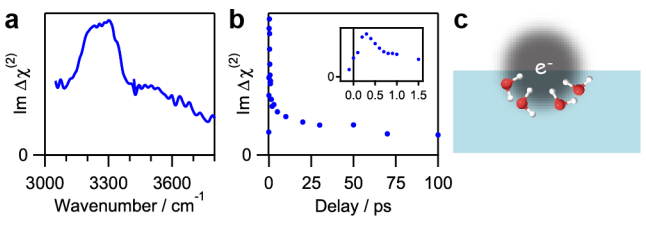

Figure 4. Analysis of the transient spectra at the air/water interface. (a) Spectrum averaged over all the delay time, (b) temporal change, and (c) assignment of the observed transient species.

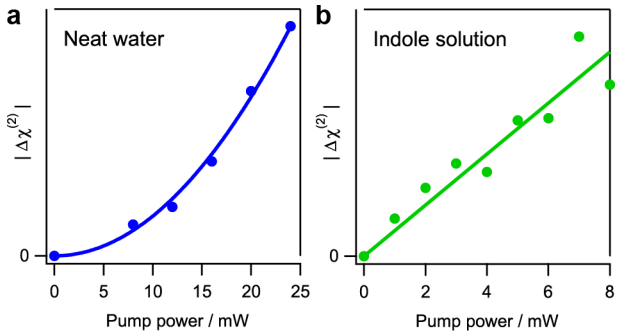

Figure 5. Power dependence of the transient signal intensity, which was extracted by fitting the complex $\Delta\chi^{(2)}$ spectra with a complex Lorentzian. (a) At the air/water interface. The intensity of the 3260 cm^{-1} band at the delay of 0.2 ps was evaluated. (b) At the air/indole solution interface. The intensity of the 3230 cm^{-1} band at the delay of 10 ps was evaluated.

intensity of the 3260 cm^{-1} band at each power, which was extracted by fitting the complex $\chi^{(2)}$ spectrum with a complex Lorentzian function. The data points are fitted well with a quadratic function as shown by the solid curve, which is consistent with eq 1. We stress that this transient signal is not due to the heat generated by the two-photon absorption of the UV-pump light. The transient spectrum of the water interface due to the heating effect has been observed in IR-pump time-resolved HD-VSFG studies.[20,24] In such a case, the transient spectrum shows a negative band and a positive band in the high- and low-frequency parts of the OH stretch region, respectively. This spectral feature arises because the heat induces a temperature increase of the water surface, which weakens the hydrogen bonding of the interfacial water and gives rise to a high-frequency shift of the negative hydrogen-bonded OH stretch band. The intensity of this transient feature is rather low; it is less than 10% of the steady-state signal intensity. In sharp contrast, the transient spectra in Figure 3 only exhibit a clear positive band on a broad offset, and the spectral feature is completely different from the transient signal arising from the heating effect. Furthermore, the intensity of the observed transient signal is very high ($(0.5-1) \times 10^{-22}$ m^2 V^{-1}, depending on the experimental condition), and it is comparable to the steady-state signal intensity, although it is expected that the two-photon absorption of the 267 nm pump light used in the present study is much less efficient than the one-photon absorption of the IR pump light used in the IR-pump time-resolved HD-VSFG study. Therefore, we can safely conclude that the transient signal observed in this study is not due to the sample heating but arises from transient species generated by the two-photon ionization of water.

As shown in eq 1, two-photon ionization of water generates not only an electron but also a hydroxyl radical (OH) and a hydronium cation (H_3O^+). The contribution of the hydronium cation to the 3260 cm^{-1} band can be easily ruled out because the observed spectrum is clearly different from the broad negative spectrum of hydronium cation at the air/water interface reported in the literature.[33] In order to make an unambiguous assignment, we carried out a time-resolved HD-VSFG experiment at the air/indole aqueous solution interface as described in the next section. The experiment clearly shows that the transient band is attributable to the electron at the water surface, not to the hydroxyl radical.

DOI: 10.1021/jacs.6b02171
J. Am. Chem. Soc. 2016, 138, 7551−7557

Air/Indole Solution Interface. The steady-state Im $\chi^{(2)}$ spectrum of the air/indole solution interface is shown in Figure 2b. The spectrum shows a high similarity to the spectrum of the air/water interface (Figure 2a), indicating that the orientation of water molecules at the interface is not drastically altered. Nevertheless, the observed bands are broader at the air/indole solution interface, suggesting that the interfacial water structure is perturbed to a certain extent by the indole molecules at this interface. More directly, a sharp negative band at ~3065 cm^{-1} in the Im $\chi^{(2)}$ spectrum is assigned to an aromatic CH stretch mode of indole,[34] indicating a substantial population of indole molecules at the surface. In fact, it is estimated from the surface pressure measurement that as many as ~5 indole molecules exist within every 1 nm^2 of the sample surface (Supporting Information). We note that the water molecules can contribute to the Im $\chi^{(2)}$ spectrum even if they are located below indole molecules, provided that they have a particular alignment due to the anisotropic environment at the interface. The positive "free OH-like" band around 3600 cm^{-1} can arise from such water molecules because indole molecules do not have an OH group and the water molecules cannot form a hydrogen bond with them. Nevertheless, a small frequency shift or broadening of such an OH stretch band is expected due to the weak interaction between the OH group and indole molecules, and actually, the "free OH-like" band at the air/indole solution interface is broader than the free OH band at the air/water interface. Such a "free OH-like" band is often called a "hydrophobic" OH band in the literature.[18,35]

At this air/indole solution interface, the electrons are generated through the one-photon ionization of indole:[5]

$$\text{indole} \xrightarrow{h\nu} S_1\ \text{indole} \rightarrow (\text{indole cation})^+ + e^- \qquad (2)$$

Figure 6 shows the UV-excited time-resolved interface-selective Im $\Delta\chi^{(2)}$ spectra in the OH stretch region at the air/indole solution interface. In contrast to the simple transient spectra at the air/water interface, complicated transient spectra are observed: The spectra show a negative feature at around 3230 cm^{-1} and a positive one at approximately 3500 cm^{-1}. Although the positive and negative features persist for more than 300 ps, the time-resolved spectra show a significant spectral change in the first 100 ps, i.e., the low-frequency side of the positive band disappears (as indicated by the broken line) and the band becomes much narrower. After this initial spectral change, the transient spectra show no further changes. This spectral change indicates that the time-resolved spectra are due to two transient species: the short-lifetime transient is depleted in the first 100 ps whereas the other remains at the interface for more than 300 ps.

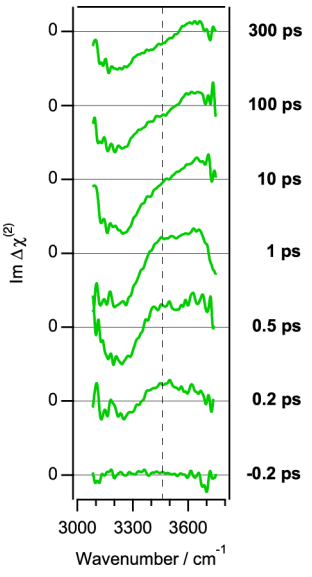

Figure 6. Time-resolved Im $\chi^{(2)}$ spectra (Im $\Delta\chi^{(2)}$) of the air/indole solution interface. The spectrum at −0.2 ps provides an estimate of the noise in our spectra. The broken line indicates the location of the quickly decaying band.

Using singular value decomposition (SVD) analysis,[36] we determined the spectra and the temporal profiles of the two transient species as shown in Figure 7, panels a, b, d, and e.

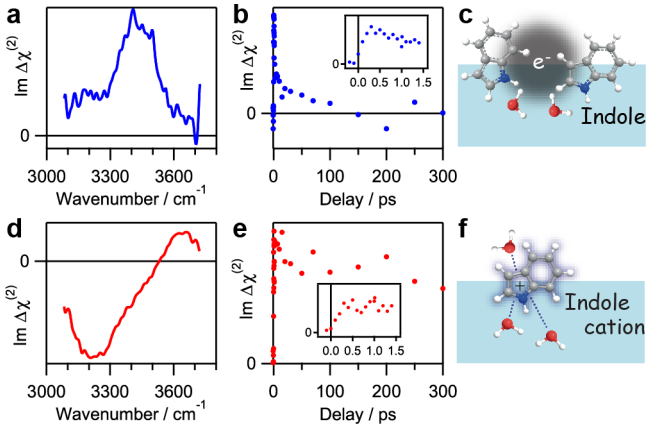

Figure 7. Analysis of the transient spectra at the air/indole solution interface. (a,d) Spectra, (b,e) temporal changes, and (c,f) assignments of the short-lived and long-lived transient species, respectively, observed at the air/indole solution interface.

SVD is a mathematical technique to decompose a set of transient spectra into the linear combination of the products of spectral basis functions and temporal basis functions that are orthonormal to each other. This decomposition is a purely mathematical process and those basis functions do not have physical significance by themselves. However, we can convert them into physically meaningful spectra and temporal profiles of real chemical species by applying several assumptions that add physical significance to this analysis. Figure 7a,b,d,e shows the final results we obtained after this conversion. The details of the analysis are given in the Supporting Information.

The analysis clearly shows that the short-lifetime transient is depleted within 100 ps in a nonexponential manner (Figure 7b) whereas the long-lifetime transient does not show a significant decay up to 300 ps (Figure 7e). More importantly, the spectrum and the decay process of the short-lifetime transient (Figure 7a,b) highly resemble those at the air/water interface (Figure 4a,b): Both spectra show a positive and relatively narrow band, and the kinetics are almost identical. These similarities allow us to have a direct comparison between the two systems, and they strongly indicate that the two spectral components are assignable to the same transient species. To confirm that the transient species at the air/indole solution interface are generated by eq 2, we evaluated the pump power dependence of the intensity of the transient band in the same manner as for the air/water interface. As shown in Figure 5b, it exhibits a linear power dependence, which unambiguously indicates that the transient bands are due to the transient

DOI: 10.1021/jacs.6b02171
J. Am. Chem. Soc. 2016, 138, 7551−7557

species generated by one-photon ionization of indole. This means that the same transient species is generated by the two different reaction schemes at the air/water and air/indole solution interfaces. Because the electron is the only transient species that is generated in both of the schemes, the two transient bands, i.e., 3260 cm^{-1} at the air/water interface and 3430 cm^{-1} at the air/indole solution interface, are attributed to the OH stretch vibration of the water molecules that directly interact with the electrons at the interface. This is reminiscent of the resonance Raman study of hydrated electrons in bulk water, where the OH stretch vibration of the water molecules that solvate the electrons is observed as a broad band centering at 3170 cm^{-1}.[37]

We note that the frequency of the transient band assigned to the hydrated electrons is noticeably different between the air/water and air/indole solution interfaces. We consider that the difference is caused by the presence/absence of indole molecules at the interface. At the air/indole solution interface, the interaction between the electron and the water molecules is weakened by indole molecules, giving rise to a higher OH stretch vibrational frequency (Figure 7c). In fact, a theoretical study of the system comprised of indole, water, and electron suggests that not only water molecules but also indole molecules may exist in the first solvation shell of the electron.[38] Such indole molecules would perturb the distribution of the electron in the vicinity of the water molecules. Thus, it is reasonable that the indole molecules affect the strength of the interaction between electrons and water molecules, which results in the frequency shift of the OH stretch vibration. We also note that transient band is accompanied by a broad positive offset-like signal (Figure 4a and 7a). This broad feature may be caused by the vibrationally nonresonant and electronically resonant SFG of the hydrated electrons. Although the wavelength for the electronic transition of hydrated electrons at the interface is not known, it is possible that the signal due to the electronic transition is detected in the present measurement because the ω_1 and $\omega_1+\omega_2$ wavelengths are close to the electronic transition wavelength of the hydrated electron in bulk water at 720 nm.[2] It is noted that an SHG study claims that they detected hydrated electrons at the air/water interface by probing the electronic transition at 700 nm.[12]

Another transient species with a long lifetime is observed at the air/indole solution interface (Figure 7d,e). Because the decay of the short-lifetime transient (i.e., hydrated electrons) is not accompanied by the rise of this long-lifetime species, the two transients are independently generated at the interface. Remembering that the electron, the S_1 indole, and the indole cation are generated at this interface (eq 2) and that the short-lifetime transient is ascribed to the hydrated electron, the long-lifetime component should be associated with the S_1 indole or the indole cation. Actually, the transient spectrum of the long-lifetime species is similar to the steady-state spectra of air/water interfaces covered with a monolayer of cationic surfactant.[17] Therefore, this component is assignable to the water molecules interacting with the indole cations at the interface (Figure 7f).

Electron Hydration at the Air/Water Interface. Time-resolved interface-selective vibrational spectroscopy enabled us to measure the vibrational spectrum of the hydrated electrons at the air/water interface. By comparing this spectrum with the spectra of water anion clusters in the gas phase and of hydrated electrons in bulk water, we can discuss a molecular-level picture of the hydrated electrons at the water surface.

In the gas phase, water anion clusters have been intensively studied as a model of hydrated electrons.[39] Figure 8a shows the

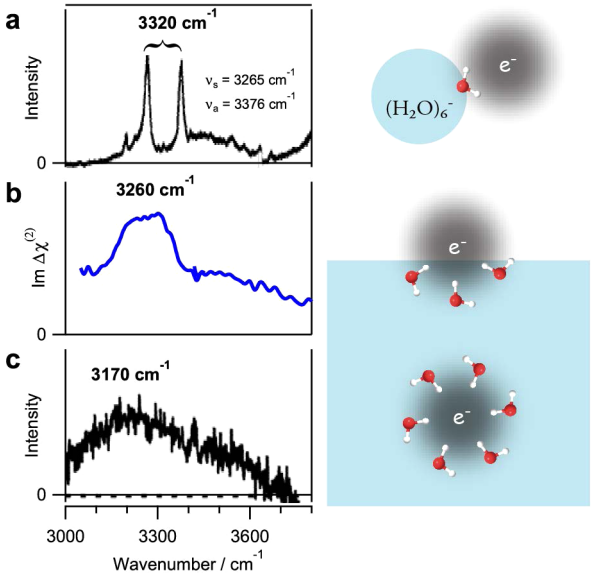

Figure 8. (a) IR spectrum of $(H_2O)_6^-$ cluster.[40] [Reprinted with permission from Hammer, N. I., et al. *J. Chem. Phys.* **2005**, *123*, 244311. Copyright 2005 AIP Publishing LLC.] (b) Im $\Delta\chi^{(2)}$ spectrum of the hydrated electrons at the air/water interface obtained in this study. (c) Raman spectrum of the hydrated electrons in bulk water.[37] [Reprinted with permission from Mizuno, M.; Tahara, T. *J. Phys. Chem. A* **2003**, *107*, 2411. Copyright 2003 American Chemical Society.]

IR spectrum of $(H_2O)_6^-$ clusters.[40] For this cluster, the theoretical calculation shows that the excess electron is hydrated by one water molecule at the cluster surface with two OH groups pointing toward the electron. Because the two OH groups of this water molecule are equivalent, the OH stretch modes mix and give rise to the symmetric stretch mode at 3265 cm^{-1} and the antisymmetric stretch mode at 3376 cm^{-1}. Thus, the intrinsic frequency of the individual OH stretch modes is estimated to be ~3320 cm^{-1}. On the other hand, in bulk water, it is considered that a hydrated electron consists of one electron and the surrounding (about four to six) water molecules that hydrate the electron.[41,42] Resonance Raman spectra of those hydrated electrons in bulk water have been measured,[37,43−46] and they show a very broad band centering around 3170 cm^{-1} (Figure 8c).[37] This shows that the OH stretch frequency observed at the water surface in the present study (3260 cm^{-1}) is located in between the frequencies in the gas phase (3320 cm^{-1}) and liquid phase (3170 cm^{-1}). The relationship between the OH stretch frequency and the degree of electron hydration is governed by two factors, i.e., spatial confinement and charge sharing. With higher degree of hydration, the electron is confined into a smaller region. Then, the higher charge density makes the OH group of water molecules interact more strongly with the electron, and the vibrational band shifts to lower frequency with respect to the vibrational frequency in the gas phase. On the other hand, higher degree of hydration also enables the charge of the electron to be shared by many water molecules. Then, because the charge experienced by each water molecule decreases, the band shifts to higher frequency as compared with the frequency in the gas phase. For the system consisting only of water

DOI: 10.1021/jacs.6b02171
J. Am. Chem. Soc. 2016, 138, 7551−7557

molecules and electrons, the observed OH stretch frequency is lower for the fully hydrated electrons in water (Figure 8c) than for the surface electrons in the gas phase (Figure 8a). This indicates that the former effect resulting from the spatial confinement of the charge is predominant. Therefore, the intermediate peak frequency (3260 cm^{-1}) observed at the air/water interface (Figure 8b) is considered to indicate that the electrons at the air/water interface are more hydrated than in the gas phase cluster and less hydrated than in bulk water, implying that electrons at the water surface are partially hydrated. Assuming that the presence of an electron does not change the sign of the hyperpolarizability, β, for the OH stretch mode of water, the positive sign of the observed Im $\Delta\chi^{(2)}$ band indicates that the water molecules solvating the electron have the hydrogen-up orientation.[16] Consequently, we obtain a picture of hydrated electrons at the water surface: electrons exist on top of the water surface, and they are partially hydrated from below (Figure 8).

We note that this picture of the hydrated electron at the water surface is consistent with the very high intensity of the transient OH stretch band we observed. Actually, intense OH stretch bands have been reported in the infrared spectra of small water anion clusters, $(H_2O)_n^-$.[40] As already mentioned, the excess electron is bound to the surface of the hydrogen-bond network of water molecules in those clusters, and one water molecule primarily interacts with the electron. The OH stretching motion of this water molecule significantly modulates the spatial distribution of the diffuse excess electron, which leads to a large change of the dipole moment and results in a very high infrared activity. In the VSFG process, $\chi^{(2)}$ is proportional to the product of the infrared activity and the Raman activity. Because a large change of the electron spatial distribution can also induce a large change of the polarizability (i.e., Raman activity), it is expected that the OH stretch vibration of the water molecule interacting with the excess electron has very large $\chi^{(2)}$. Therefore, the intense transient OH stretch band in the Im $\Delta\chi^{(2)}$ spectra is expected for partially hydrated electrons at the water surface because the spatial distribution of the electron, in particular the part of electron protruding into the air, can be largely modulated with the OH stretch vibration of the water molecules that interact with the electron.

The present study also shows that the hydrated electrons are not very stable at the interface and disappear from the interface within 100 ps (Figures 4b and 7b). Because the decay dynamics of the hydrated electrons are almost the same at the air/water and air/indole solution interfaces, and because the indole cations stay at the interface for a much longer time than the hydrated electrons (Figure 7e), the disappearance of the partially hydrated electrons is not due to the recombination between the electron and the cation. Rather, the partially hydrated electrons escape into the bulk water to become fully hydrated. This view is in excellent agreement with the conclusion obtained by a previous molecular dynamics (MD) simulation[47] which predicts that electrons at the water surface escape into the bulk on a 10 ps time scale. It is noteworthy that, in another MD simulation study, Uhlig et al. claim that the electrons are fully hydrated at the air/water interface.[48] However, the simulated electron distribution actually shows that some part of the electron distribution protrudes into the air, which means that the electrons are "partially hydrated" in our terminology.

CONCLUSION

Using novel time-resolved and interface-selective vibrational spectroscopy, we obtained for the first time the vibrational spectrum of hydrated electrons at the air/water interface. Based on the obtained vibrational spectrum, we concluded that the electron at the water surface is only partially hydrated. Furthermore, we observed that this partially hydrated state of an electron is not very stable and that the electron escapes into bulk water within 100 ps to become fully hydrated.

Although the selective observation of short-lived transient species at liquid interfaces is an experimentally challenging task, we have demonstrated that UV-excited time-resolved HD-VSFG spectroscopy can achieve this. The application of this new method is not limited to hydrated electrons but can be utilized to study the dynamics of various chemical processes at liquid interfaces. UV-excited time-resolved HD-VSFG spectroscopy is a promising technique that provides new insights into interfacial chemical reactions.

ASSOCIATED CONTENT

Supporting Information

The Supporting Information is available free of charge on the ACS Publications website at DOI: 10.1021/jacs.6b02171.

Supplementary discussion, including figures and equations (PDF)

AUTHOR INFORMATION

Corresponding Author

*tahei@riken.jp

Present Addresses

[⊥]K.M.: Max Planck Institute for the Science of Light, Günther-Scharowsky-Straße 1, 91058 Erlangen, Germany

[∥]R.K.: Nuclear Science and Engineering Center, Japan Atomic Energy Agency (JAEA), Tokai-mura, Ibaraki 319-1195, Japan

[#]S.Y.: Department of Applied Chemistry, Graduate School of Science and Engineering, Saitama University, 255 Shimo-Okubo, Sakura-ku, Saitama 338−8570, Japan

Notes

The authors declare no competing financial interest.

ACKNOWLEDGMENTS

This work was supported by JSPS KAKENHI Grant numbers JP24245006, JP25104005. R.K. acknowledges the Special Postdoctoral Researchers (SPDR) program of RIKEN.

REFERENCES

(1) Hart, E. J.; Boag, J. W. *J. Am. Chem. Soc.* **1962**, *84*, 4090.

(2) Nikogosyan, D. N.; Oraevsky, A. A.; Rupasov, V. I. *Chem. Phys.* **1983**, *77*, 131.

(3) Alfano, J. C.; Walhout, P. K.; Kimura, Y.; Barbara, P. F. *J. Chem. Phys.* **1993**, *98*, 5996.

(4) Shi, X.; Long, F. H.; Lu, H.; Eisenthal, K. B. *J. Phys. Chem.* **1996**, *100*, 11903.

(5) Peon, J.; Hess, G. C.; Pecourt, J.-M. L.; Yuzawa, T.; Kohler, B. *J. Phys. Chem. A* **1999**, *103*, 2460.

(6) Laenen, R.; Roth, T.; Laubereau, A. *Phys. Rev. Lett.* **2000**, *85*, 50.

(7) Kambhampati, P.; Son, D. H.; Kee, T. W.; Barbara, P. F. *J. Phys. Chem. A* **2002**, *106*, 2374.

(8) Larsen, R. E.; Glover, W. J.; Schwartz, B. J. *Science* **2010**, *329*, 65.

(9) Turi, L.; Rossky, P. J. *Chem. Rev.* **2012**, *112*, 5641.

(10) Garrett, B. C.; Dixon, D. A.; Camaioni, D. M.; Chipman, D. M.; Johnson, M. A.; Jonah, C. D.; Kimmel, G. A.; Miller, J. H.; Rescigno, T. N.; Rossky, P. J.; Xantheas, S. S.; Colson, S. D.; Laufer, A. H.; Ray,

DOI: 10.1021/jacs.6b02171
J. Am. Chem. Soc. 2016, 138, 7551−7557

D.; Barbara, P. F.; Bartels, D. M.; Becker, K. H.; Bowen, K. H.; Bradforth, S. E.; Carmichael, I.; Coe, J. V.; Corrales, L. R.; Cowin, J. P.; Dupuis, M.; Eisenthal, K. B.; Franz, J. A.; Gutowski, M. S.; Jordan, K. D.; Kay, B. D.; LaVerne, J. A.; Lymar, S. V.; Madey, T. E.; McCurdy, C. W.; Meisel, D.; Mukamel, S.; Nilsson, A. R.; Orlando, T. M.; Petrik, N. G.; Pimblott, S. M.; Rustad, J. R.; Schenter, G. K.; Singer, S. J.; Tokmakoff, A.; Wang, L.-S.; Zwier, T. S. *Chem. Rev.* **2004**, *105*, 355.
(11) Siefermann, K. R.; Liu, Y.; Lugovoy, E.; Link, O.; Faubel, M.; Buck, U.; Winter, B.; Abel, B. *Nat. Chem.* **2010**, *2*, 274.
(12) Sagar, D. M.; Bain, C. D.; Verlet, J. R. R. *J. Am. Chem. Soc.* **2010**, *132*, 6917.
(13) Buchner, F.; Schultz, T.; Lubcke, A. *Phys. Chem. Chem. Phys.* **2012**, *14*, 5837.
(14) Nihonyanagi, S.; Mondal, J. A.; Yamaguchi, S.; Tahara, T. *Annu. Rev. Phys. Chem.* **2013**, *64*, 579.
(15) Shen, Y. R. *Annu. Rev. Phys. Chem.* **2013**, *64*, 129.
(16) Nihonyanagi, S.; Yamaguchi, S.; Tahara, T. *J. Chem. Phys.* **2009**, *130*, 204704.
(17) Nihonyanagi, S.; Yamaguchi, S.; Tahara, T. *J. Am. Chem. Soc.* **2010**, *132*, 6867.
(18) Mondal, J. A.; Nihonyanagi, S.; Yamaguchi, S.; Tahara, T. *J. Am. Chem. Soc.* **2012**, *134*, 7842.
(19) Nihonyanagi, S.; Yamaguchi, S.; Tahara, T. *J. Am. Chem. Soc.* **2014**, *136*, 6155.
(20) Nihonyanagi, S.; Singh, P. C.; Yamaguchi, S.; Tahara, T. *Bull. Chem. Soc. Jpn.* **2012**, *85*, 758.
(21) Singh, P. C.; Nihonyanagi, S.; Yamaguchi, S.; Tahara, T. *J. Chem. Phys.* **2012**, *137*, 094706.
(22) Singh, P. C.; Nihonyanagi, S.; Yamaguchi, S.; Tahara, T. *J. Chem. Phys.* **2013**, *139*, 161101.
(23) Singh, P. C.; Nihonyanagi, S.; Yamaguchi, S.; Tahara, T. *J. Chem. Phys.* **2014**, *141*, 18C527.
(24) Inoue, K.; Nihonyanagi, S.; Singh, P. C.; Yamaguchi, S.; Tahara, T. *J. Chem. Phys.* **2015**, *142*, 212431.
(25) Xiong, W.; Laaser, J. E.; Mehlenbacher, R. D.; Zanni, M. T. *Proc. Natl. Acad. Sci. U. S. A.* **2011**, *108*, 20902.
(26) Laaser, J. E.; Skoff, D. R.; Ho, J.-J.; Joo, Y.; Serrano, A. L.; Steinkruger, J. D.; Gopalan, P.; Gellman, S. H.; Zanni, M. T. *J. Am. Chem. Soc.* **2014**, *136*, 956.
(27) Hsieh, C.-S.; Okuno, M.; Hunger, J.; Backus, E. H. G.; Nagata, Y.; Bonn, M. *Angew. Chem., Int. Ed.* **2014**, *53*, 8146.
(28) Yamaguchi, S.; Tahara, T. *J. Chem. Phys.* **2008**, *129*, 101102.
(29) Nihonyanagi, S.; Ishiyama, T.; Lee, T.-k.; Yamaguchi, S.; Bonn, M.; Morita, A.; Tahara, T. *J. Am. Chem. Soc.* **2011**, *133*, 16875.
(30) Nihonyanagi, S.; Kusaka, R.; Inoue, K.; Adhikari, A.; Yamaguchi, S.; Tahara, T. *J. Chem. Phys.* **2015**, *143*, 124707.
(31) Ji, N.; Ostroverkhov, V.; Tian, C.; Shen, Y. *Phys. Rev. Lett.* **2008**, *100*, 096102.
(32) Yamaguchi, S. *J. Chem. Phys.* **2015**, *143*, 034202.
(33) Tian, C.; Ji, N.; Waychunas, G. A.; Shen, Y. R. *J. Am. Chem. Soc.* **2008**, *130*, 13033.
(34) Majoube, M.; Vergoten, G. *J. Raman Spectrosc.* **1992**, *23*, 431.
(35) Ma, G.; Chen, X.; Allen, H. C. *J. Am. Chem. Soc.* **2007**, *129*, 14053.
(36) Yamaguchi, S.; Hamaguchi, H. *J. Chem. Phys.* **1998**, *109*, 1397.
(37) Mizuno, M.; Tahara, T. *J. Phys. Chem. A* **2003**, *107*, 2411.
(38) Jalbout, A. F.; Hall, C. S.; Adamowicz, L. *J. Chem. Phys.* **2003**, *118*, 10541.
(39) Neumark, D. M. *Mol. Phys.* **2008**, *106*, 2183.
(40) Hammer, N. I.; Roscioli, J. R.; Bopp, J. C.; Headrick, J. M.; Johnson, M. A. *J. Chem. Phys.* **2005**, *123*, 244311.
(41) Kevan, L. *Acc. Chem. Res.* **1981**, *14*, 138.
(42) Jacobson, L. D.; Herbert, J. M. *J. Chem. Phys.* **2010**, *133*, 154506.
(43) Mizuno, M.; Tahara, T. *J. Phys. Chem. A* **2001**, *105*, 8823.
(44) Mizuno, M.; Yamaguchi, S.; Tahara, T. *J. Phys. Chem. A* **2005**, *109*, 5257.
(45) Tauber, M. J.; Mathies, R. A. *J. Phys. Chem. A* **2001**, *105*, 10952.
(46) Tauber, M. J.; Mathies, R. A. *J. Am. Chem. Soc.* **2003**, *125*, 1394.
(47) Madarasz, A.; Rossky, P. J.; Turi, L. *J. Chem. Phys.* **2007**, *126*, 234707.
(48) Uhlig, F.; Marsalek, O.; Jungwirth, P. *J. Phys. Chem. Lett.* **2013**, *4*, 338.

DOI: 10.1021/jacs.6b02171
J. Am. Chem. Soc. 2016, 138, 7551−7557